

# Percolation of linear $k$ -mers on a square lattice: From isotropic through partially ordered to completely aligned states

Yuri Yu. Tarasevich\*

*Astrakhan State University, 20a Tatishchev Street, 414056 Astrakhan, Russia*

Nikolai I. Lebovka†

*Institute of Biocolloidal Chemistry named after F.D. Ovcharenko, NAS of Ukraine, 42, Boulevard Vernadskogo, 03142 Kiev, Ukraine*

Valeri V. Laptev‡

*Astrakhan State Technical University, 16 Tatishchev Street, 414025 Astrakhan, Russia and**Astrakhan State University, 20a Tatishchev Street, 414056 Astrakhan, Russia*

(Received 17 August 2012; published 12 December 2012)

Numerical simulations by means of Monte Carlo method and finite-size scaling analysis have been performed to study the percolation behavior of linear  $k$ -mers (also denoted in publications as rigid rods, needles, sticks) on two-dimensional square lattices  $L \times L$  with periodic boundary conditions. Percolation phenomena are investigated for anisotropic relaxation random sequential adsorption of linear  $k$ -mers. Especially, effect of anisotropic placement of the objects on the percolation threshold has been investigated. A detailed study of the behavior of percolation probability  $R_L(p)$  that a lattice of size  $L$  percolates at concentration  $p$  in dependence on  $k$ , anisotropy, and lattice size  $L$  has been performed. A nonmonotonic size dependence for the percolation threshold has been confirmed in the isotropic case. We propose a fitting formula for percolation threshold,  $p_c = a/k^\alpha + b \log_{10} k + c$ , where  $a$ ,  $b$ ,  $c$ , and  $\alpha$  are the fitting parameters depending on anisotropy. We predict that for large  $k$ -mers ( $k \gtrsim 1.2 \times 10^4$ ) isotropically placed at the lattice, percolation cannot occur, even at jamming concentration.

DOI: 10.1103/PhysRevE.86.061116

PACS number(s): 64.60.ah, 64.60.De, 68.35.Rh, 61.43.Bn

## I. INTRODUCTION

Percolation deals with the properties of disordered media. Such media can be composed of the objects placed in a space. The objects can connect with each other and form clusters. If object concentration is large enough, infinitely large cluster occurs. Such a concentration is known as a percolation threshold. The properties of media are considerably different below and above percolation threshold. If objects are placed in a space purely at random, the percolation is called random or Bernoulli percolation. Moreover, different correlations or constraints may be applied to the space distribution of the objects. The media composed in such a way may be partially disordered and anisotropic. Very often, a discrete space (lattice) is utilized to simplify consideration. In this case, the cluster-forming objects are sites of the lattice. Percolation of the point objects (singly occupied site) on different lattices in plane and multidimensional space is more intensively studied. Percolation of the objects occupying several nearest sites is studied significantly less. The examples of such objects are linear, cyclic, and branched  $k$ -mers, i.e.,  $k$  nearest sites. The numerous publications are devoted to both theoretical and applied aspects of percolation (see, e.g., Refs. [1–3]). During the past few decades, percolation of the anisotropic penetrable and impenetrable objects (rods, sticks, linear  $k$ -mers, ellipsoids, etc.) has been intensively investigated. Our overview is restricted to the works devoted to the percolation of linear objects on a lattice.

Mainly, the studies are devoted to the isotropic problem on a square lattice when the  $k$ -mers with horizontal and vertical orientations are deposited with equal probability. A computer simulation model for linear  $k$ -mers ( $k = 1 \dots 20$ ) showed that percolation threshold  $p_c$  decreases with increasing of the chain-length  $k$  as  $1/k^{0.5}$  [4]. The percolation exponents (order parameter, susceptibility, and correlation length exponents) seemed to remain unchanged.

The study of the percolative properties of systems generated by a random sequential adsorption (RSA) of  $k$ -mers ( $k = 1 \dots 40$ ) have been performed by Leroyer and Pommiers [5]. They have demonstrated that as the segment length grows, the percolation threshold  $p_c$  decreases, goes through a minimum, and then increases slowly for large  $k$  ( $k \geq 16$ ).

Later on, Kondrat and Pękalski [6] extended the studies percolation and jamming of the same problem to the  $k$ -mer length in the interval  $k = 1 \dots 2000$ . The authors have shown that the jamming threshold decreases monotonically approaching the asymptotic value of  $p_j = 0.66 \pm 0.01$  at large  $k$ , and percolation threshold  $p_c$  is a nonmonotonic function of the length  $k$ , with a minimum for a certain length of the  $k$ -mers ( $k = 13$ ). However, these results for very large needles cannot be treated as accurate because of moderate size of the studied lattices ( $L \leq 2500$ ) and possibility of large finite-size corrections.

The details of the monotonic behavior of the percolation threshold for small  $k$ -mer length ( $k \leq 15$ ) have been widely discussed in literature [7–10]. Percolation and jamming phenomena have been investigated for  $k$ -mer length within the interval  $k = 1 \dots 10$  by Vandewalle *et al.* [7]. The authors conjectured presence of a universal connection in geometry of jamming and percolation that resulted in constancy of the ratio of percolation and jamming concentration  $p_c/p_j$  ( $\simeq 0.62$ ) for

\*tarasevich@aspu.ru

†lebovka@gmail.com

‡serpentvv@mail.ru

all sizes of  $k$ -mers. The following equation for the percolation threshold as a function of  $k$ -mer length has been proposed

$$p_c = C \left[ 1 - \gamma \left( \frac{k-1}{k} \right)^2 \right], \quad (1)$$

where  $C$  and  $\gamma$  are the constants.

Cornette *et al.* [8] have performed the finite-size scaling tests and shown that the  $k$ -mer problem in all the studied cases belongs to the random percolation universality class. They fitted the data for the  $k$ -mers ( $k = 1 \dots 15$ ) with the following exponential equation:

$$p_c = p_c^\infty + \Omega \exp\left(-\frac{k}{\kappa}\right), \quad (2)$$

where  $p_c^\infty = 0.461 \pm 0.001$ ,  $\Omega = 0.197 \pm 0.02$ , and  $\kappa = 2.775 \pm 0.02$  are the fitting parameters.  $p_c^\infty$  is the expected value in the limit  $k \rightarrow \infty$ .

Recently, these problems have been extended for partially ordered  $k$ -mer (when the particles with horizontal and vertical orientations can be deposited with unequal probability) [11–13]. The effect of dimer alignment on percolation and jamming phenomena on a square lattice has been investigated by Cherkasova *et al.* [11]. The influence of dimer alignment on the electrical conductivity has been also examined. The effect of  $k$ -mer alignment on the jamming threshold has been extensively examined for the  $k$  in the interval  $1 \dots 256$  [12]. The percolation behavior for the  $k$ -mer length in the interval  $k = 1 \dots 15$  has been studied recently by Longone *et al.* [13]. Only two particular cases have been studied in the work, i.e., the isotropic case and the completely ordered case (all  $k$ -mers are aligned along the given direction). In both cases, the percolation threshold is the monotonic decreasing function of the  $k$ -mer length  $k$ .

Most recent numerical studies have been devoted to the analysis of equilibrium properties in systems of  $k$ -mers [14–17]. The equilibrium systems have been simulated using the deposition-evaporation dynamics. The studies showed existence of an orientationally ordered phase (nematic phase) for long  $k$ -mers. The universality class for the percolation and isotropic-nematic phase transition has been found to be the same as of the random percolation and Ising models. The nonmonotonic size dependence has been observed for the percolation threshold of unaligned  $k$ -mers; it goes through a minimum at  $k \simeq 5$  and asymptotically converges toward a definite value of  $p_c \simeq 0.54$  for large, fully aligned  $k$ -mers [18]. It has been interpreted as a consequence of the isotropic-nematic phase transition occurring in the system for large values of  $k$ .

Except purely theoretical interest, such considerations may have different applications. For instance, the percolation approach is suitable to describe physical and chemical properties of monolayers formed during adsorption of the polymer chains [19]. Another possible application is connected with the nanotechnologies (see, e.g., Ref. [20]). Recently, the current progress in the production of aligned single-walled carbon nanotubes (SWCNTs) has been reviewed by Ma *et al.* [21]. The semiempirical theories of composites containing randomly oriented anisotropic inclusions (needle, prolate or oblate spheroid, sphere, or disk) have been developed

and they are useful for prediction of effective electrical or thermal conductivities of multiwalled carbon nanotube composites [20,22–25]. The first experiments evidenced the lowering of the threshold in comparison with isotropic systems [26]. The experiments for random stick patterns obtained by photolithographic techniques supported the universality hypothesis for 2D systems [27]. The universality concept has been also confirmed in experiments with the aluminum film containing the insulating ellipsoids with the same direction of the major axis [28].

This work discusses the percolation behavior of linear  $k$ -mers on square lattice with different degrees of alignment characterized by order parameter. We try to shed light on the uncertainty in question about the presence or absence the nonmonotonic  $k$ -dependence for the percolation threshold by studying the systems with  $k$  varying from 1 up to 512.

In our work, we try to find the answers to the questions listed below

(1) Are Eqs. (1) and (2) valid for very long linear objects or do they work only for rather short objects?

(2) How does anisotropic placement of the objects effect the percolation threshold?

The rest of paper is arranged as follow. In Sec. II, we describe our model and the details of simulation. The obtained results are discussed in Sec. III. We summarize the results and conclude our paper in Sec. IV.

## II. DESCRIPTION OF MODELS AND DETAILS OF SIMULATIONS

The problem of linear  $k$ -mers, where  $k = 2^n$  and  $n = 1, 2, \dots, 9$ , on the square lattices of  $L \times L$  size has been studied. Linear lattice size,  $L$ , varies from 100 to 19 200 in different simulations. Periodic boundary conditions in vertical and horizontal directions have been applied, i.e., percolation on a torus has been considered.

### A. Filling of the lattice by $k$ -mers

The relaxation random sequential adsorption (RRSA) model [12] has been used to place the  $k$ -mers on a lattice. In this model, there is an infinitely large reservoir filled with  $k$ -mers oriented with given and fixed anisotropy. The  $k$ -mer is taken from the reservoir and an attempt of its deposition is carried out starting from a lattice site selected at random until the object is deposited. In contrast with the conventional random sequential adsorption (RSA) model, when any unsuccessful attempt is rejected and another object is selected for deposition, the RRSA model ensures that anisotropy of the deposit is the same as the anisotropy of the objects suspended in the reservoir [12].

The degree of anisotropy is characterized by the order parameter  $s$  defined as

$$s = \left| \frac{N_+ - N_-}{N_+ + N_-} \right|, \quad (3)$$

where  $N_+$  and  $N_-$  are the numbers of  $k$ -mers oriented in vertical and horizontal directions, respectively.

For isotropic system,  $s = 0$ , the quantity of vertical and horizontal  $k$ -mers are the same, and for totally aligned system,

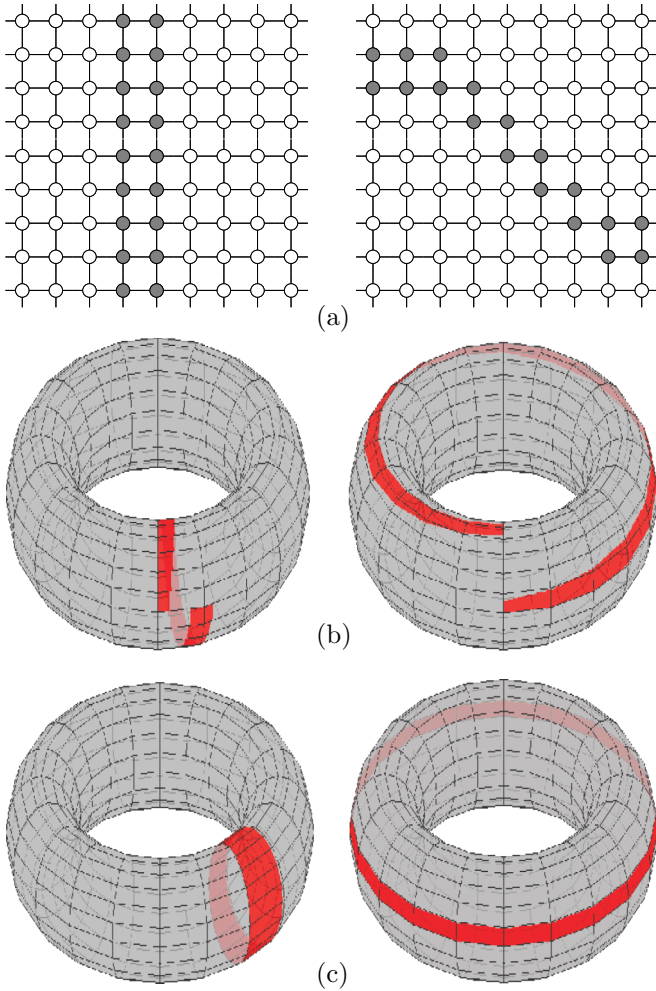


FIG. 1. (Color online) Percolating clusters of different sorts on a plane and on a torus. (a) Crossing clusters; (b) spiral-like wrapping clusters; (c) ringlike wrapping clusters.

$s = 1$ , all  $k$ -mers are aligned in vertical direction. For these two marginal cases, RRSA and RSA models are absolutely identical [12].

The Mersenne twister random number generator [29] with a period of  $2^{19937} - 1$  has been exploited to generate positions and orientations of the deposited objects.

### B. Determination of percolation threshold

A crossing cluster is determined as a cluster that connects two opposite borders of lattice with open boundary conditions. Examples of crossing clusters that percolate along vertical direction or along horizontal direction are presented in Fig. 1(a).

A wrapping cluster is determined as a cluster that winds (i.e., provides a path of length  $2\pi$ ) around the lattice with the periodic (toroidal) boundary conditions along the given direction [30]. The wrapping cluster may be either disconnected (spirallike) [Fig. 1(b)] or continuous (ringlike) [Fig. 1(c)] or more complex.

From the topological point of view, the spirallike clusters presented in Fig. 1(b) are homotopic to a point; i.e., they can be continuously deformed to a point. Hence, they significantly differ from the ringlike clusters shown in Fig. 1(c). From

the physical point of view, it is rather natural to think that applying periodic boundary conditions cannot destroy a percolating state existing in plane with open boundary conditions. Moreover, it can produce a new percolating state due to an additional kind of symmetry, i.e., translation symmetry.

In our study, a system is considered as percolating if at least one spiral cluster [Fig. 1(b)] can be found. To be certain, we call it a problem of *physical percolation on a torus* in contrast with *topological percolation* when only self-connected clusters are treated as wrapping ones [31].

The value of threshold concentration may be determined by calculation of the probability  $R_L(p)$  for a cluster to cross a square lattice of  $L \times L$  sites, if the boundary conditions are open, or to wrap around the periodic boundary conditions. In the thermodynamical limit ( $L \rightarrow \infty$ ), this probability is equal to the probability that the system percolates (i.e., it tends to the step-function and equals 0 below the percolation threshold and 1 above it) [32].

Since cluster wrapping can be defined in a number of different ways (see, e.g., Ref. [32]), there are a corresponding number of different probabilities  $R_L$ :

- (1)  $R_L^h$  is the probability of wrapping horizontally around the system;
- (2)  $R_L^v$  is the probability of wrapping vertically around the system;
- (3)  $R_L^{\text{or}}$  is the probability of wrapping around either the horizontal or vertical direction, or both;
- (4)  $R_L^{\text{and}}$  is the probability of wrapping around both directions simultaneously.

For the square lattices and isotropic problem these probabilities satisfy the following relations [32,33]:

$$R_L^h = R_L^v, \quad (4)$$

$$R_L^h = (R_L^{\text{or}} + R_L^{\text{and}})/2, \quad (5)$$

as well as the inequalities

$$R_L^{\text{and}} \leq R_L^h \leq R_L^{\text{or}}. \quad (6)$$

Equations (4) and (5) provide evidence that only two of the percolation probabilities are independent. Obviously, for an anisotropic system Eq. (4) cannot hold and, hence, there are three independent probabilities. Nevertheless, for a strong anisotropic system, a spanning or wrapping cluster always arises along one direction, say vertical, and hence,  $R^v = R^{\text{or}}$ ,  $R^h = R^{\text{and}}$ .

The detailed studies have shown [8,34] that for the specified problem (e.g., for crossing or wrapping clusters) and the criterion used, the curves  $R_L(p)$  cross each other in a unique intersection point  $R^*$  located at  $p = p_c$  in the thermodynamical limit ( $L \rightarrow \infty$ ).

Figure 2 compares  $R_L^{\text{or}}(p)$  and  $R_L^{\text{and}}(p)$  dependencies for monomer problem ( $k = 1$ ), i.e., conventional site problem, for different size of square lattice,  $L$ . The results are presented for the systems with periodic and open boundary conditions.

If the disconnected spiral clusters similar to those shown in Fig. 1(b) are not treated as percolating, the exact expressions of  $R^*$  at percolation threshold,  $p_c$ , for each of the definitions have been deduced [34] from the work by Pinson [31]. The values of  $R^*$  presented by Newman and Ziff [32,33] are  $R^{*\text{or}} = 0.690473725$ ,  $R^{*\text{and}} = 0.351642855$ .

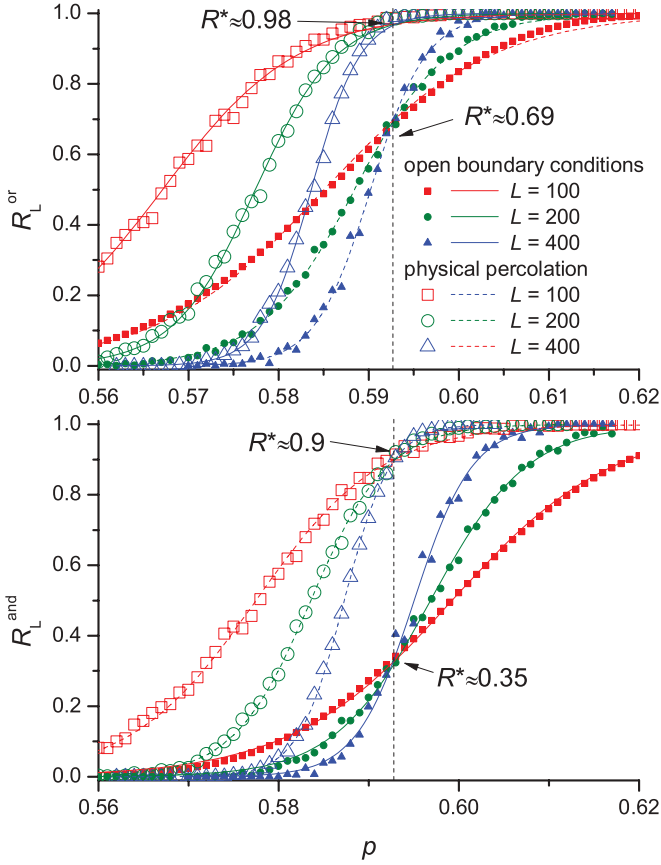


FIG. 2. (Color online) Comparison of  $R_L^{\text{or}}$  and  $R_L^{\text{and}}$  versus  $p$  dependencies for monomer problem ( $k = 1$ ) (physical percolation) and crossing clusters (with open boundary conditions) and different size of square lattice,  $L$ .

In our study, the intersection points  $R^*$  for physical percolation are  $R_L^{\text{or}} \simeq 0.90$  and  $R_L^{\text{and}} \simeq 0.98$ .

The  $R_L(p)$  functions have been estimated by performing 1 000 independent runs. Percolation concentration  $p_c(L)$  for the lattice of given linear size  $L$  filled with  $k$ -mers at the given concentration  $p$  has been determined using the fitting function [35]

$$R_L(p) = (1 + \exp\{-[p - p_c(L)]a\})^{-1}, \quad (7)$$

where  $a$  is adjusted constant.

To extrapolate the estimations of the percolation thresholds  $p_c(L)$  obtained at the lattice of size  $L$  to the infinitely large lattice  $p_c(\infty)$ , the usual finite-size scaling analysis of the percolation behavior has been done. To perform extrapolation, we used at least three lattices of different sizes and scaling relation

$$|p_c(L) - p_c(\infty)| \propto L^{-1/\nu}, \quad (8)$$

where  $\nu = 4/3$  is the critical exponent of correlation length for the 2D random percolation problem [1]. In our study, the typical values of lattice size are  $L = 50k, 75k, 100k, 150k, 200k, 400k$ .

The universality of the  $k$ -mers problem ( $s = 0$ ) has been justified before [8]. We tested validity of scaling Eq. (8) for anisotropic problem ( $s > 0$ ) (see Fig. 3 for typical sample).

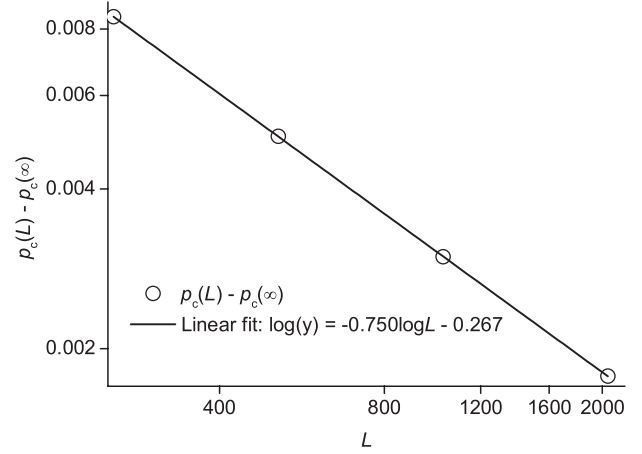


FIG. 3. Critical exponent  $\nu$  extracting for  $k = 2$ ,  $s = 0.5$ .  $\nu^{-1} = 0.750 \pm 0.001$ . Log-log scale.

Our result  $\nu^{-1} = 0.750 \pm 0.001$  is in the excellent agreement with the theoretical value  $\nu = 4/3$  [1].

Examples of  $p_c$  versus  $L$  scaling behavior for  $k = 16$ ,  $s = 0.8$ , and four criteria ( $h, v, or, and$ ) are presented in Fig. 4.

The preliminary studies have shown that in all cases the  $p_c(L)$  scaling is minimal for criterion *and*. The final results of percolation concentration have been obtained using the criterion *and*. To simplify the notation, below we omit superscript *and* where it is possible.

To avoid very time-consuming computations with the lattices of huge size for  $k = 256$  and  $s = 0$ , we used only two relatively small lattices,  $L = 50k$  and  $L = 75k$ , and two different criteria, namely *and* and *or*. Intersection points [i.e.,  $p_c(\infty)$ ] extracted from Eq. (8) for two different criteria are almost the same within error bar about 0.001.

Another special case is  $k = 512$ ,  $s = 0$ . Only one lattice size  $L = 37k$  has been used for rough estimation of the percolation threshold. Percolation concentration has been calculated from the equation  $R_L^{\text{and}}(p_c) = 0.9$ .

### C. Other details

Breadth-first search (BFS) algorithm has been applied to identify a percolation cluster. BFS seems to be faster and more appropriate for the toroidal boundary conditions than Hoshen-Kopelman (HK76) algorithm [36]. The additional tests have shown that results obtained using BFS and HK76 algorithms are identical within error bar.

The mean degree of the system anisotropy has been calculated as

$$\delta = \sum_{i=1}^{N_c} N_i \alpha_i / N_t, \quad (9)$$

where  $\alpha_i = (R_i^y - R_i^x) / R_i$ . Here,  $R_i^y$  and  $R_i^x$  are radii of gyration of cluster  $i$  in  $y$  and  $x$  directions, respectively;  $R_i$  is its mean radius of gyration,  $N_c$  is a total number of clusters,  $N_i$  is a number of filled sites in the cluster  $i$ , and  $N_t$  is a total number of the filled sites.

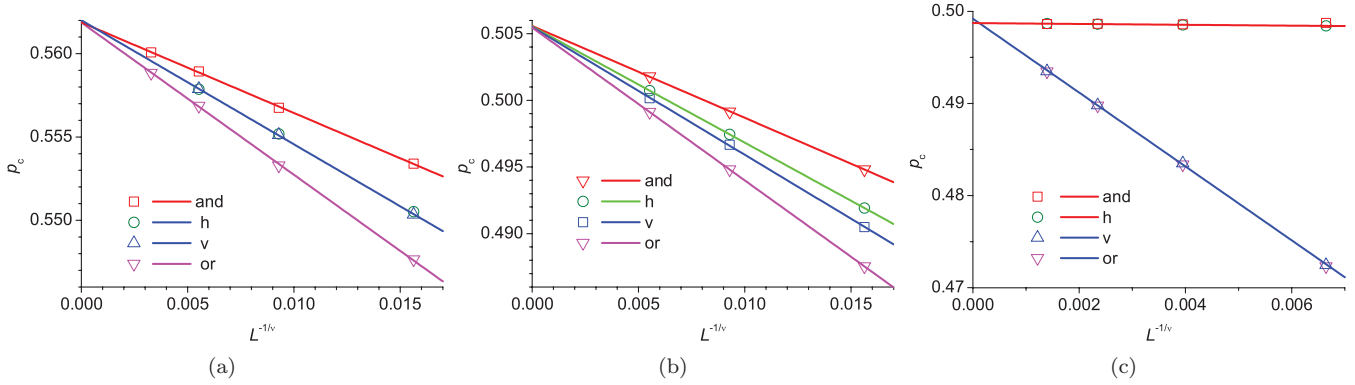


FIG. 4. (Color online) Percolation concentration  $p_c$  versus size of the lattice  $L$  for different criteria for physical percolation. (a) Isotropic case,  $k = 2$ ,  $s = 0.0$ . (b) Slightly anisotropic case,  $k = 4$ ,  $s = 0.1$ . (c) Anisotropic case,  $k = 16$ ,  $s = 0.8$ .

III. RESULTS AND DISCUSSION

A. Nonuniversality of intersection points  $R^*$

The value of the percolation probability or percolation cumulant at the intersection point  $R^*$  may be an important characteristic representing the universality class [13]. Figure 5 presents examples of percolation probability  $R_L$  versus  $k$ -mers concentration  $p$  for isotropic systems,  $s = 0$ , and different values of  $k$  and  $L$ .

For the isotropic problem, the position of the intersection point remained unchanged within precision of estimation, being  $R^* \simeq 0.90$  for all  $k$  within the interval between 1 and 512. This behavior is rather similar to that observed for percolation problem of  $k$ -mers with open boundary condition [8]. For the criterion *and*, the same values of  $R^* \simeq 0.3$  have been observed for the different length of  $k$ -mers ranging between  $k = 1$  and  $k = 25$ . Thus, universality of intersection points  $R^*$  has been observed for the systems with different boundary conditions (periodical and open) and it may indicate the conserving of universality class irrespective of the size of  $k$ -mers.

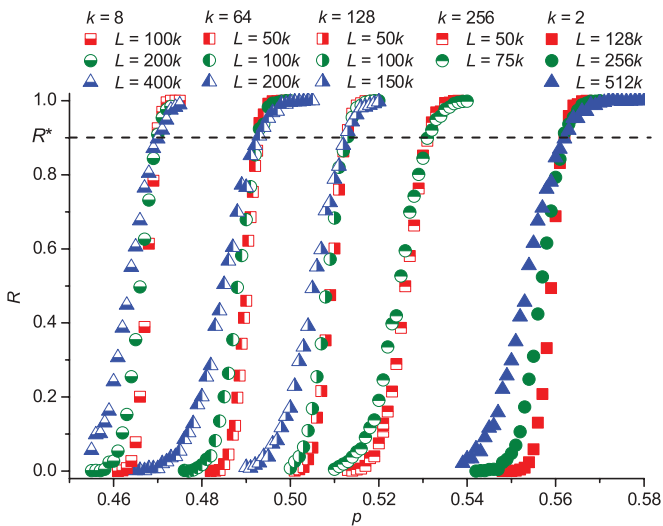


FIG. 5. (Color online) Probability curves for isotropic systems,  $s = 0$ , and different values of  $k$  and  $L$ . Arrows indicate the intersection points.

However, such universality of intersection points  $R^*$  has been not observed for anisotropic systems. Figure 6 presents examples of percolation probability  $R$  versus  $k$ -mer concentration  $p$  for  $k = 32$  and different values of  $s$  and  $L$ . At fixed value of  $k$ , the position of intersection point  $R^*$  continuously decreased with increasing of  $s$ .

The more detailed studies have shown that for anisotropic systems the position of intersection points  $R^*$  also depends on the value of  $k$  (Fig. 7). For the completely ordered systems,  $s = 1$ , the value of  $R^*$  decreased monotonically and became close to 0 for larger sizes of  $k$ -mers. This observation may reflect the continuous change of universality class and corresponds to previously reported data for the completely ordered systems with open boundary conditions [13]. For partially ordered systems, the similar effect of  $k$ -mers length on the value of  $R^*$  has been observed (Fig. 7).

Thus, orientation of  $k$ -mers affected the universality class of this percolation problem and it has been conserved only for the isotropic systems ( $s = 0$ ), where universality is the same for the different length of  $k$ -mers. It can be speculated that this violation of universality can reflect the effect of the system anisotropy. This anisotropy has been maximally denominated

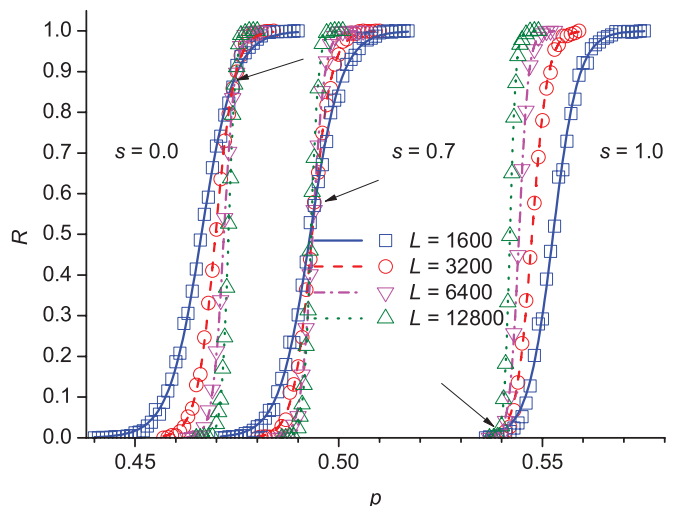


FIG. 6. (Color online) Probability curves for  $k = 32$ ,  $s = 0.0, 0.7, 1.0$ . Arrows indicate the intersection points.

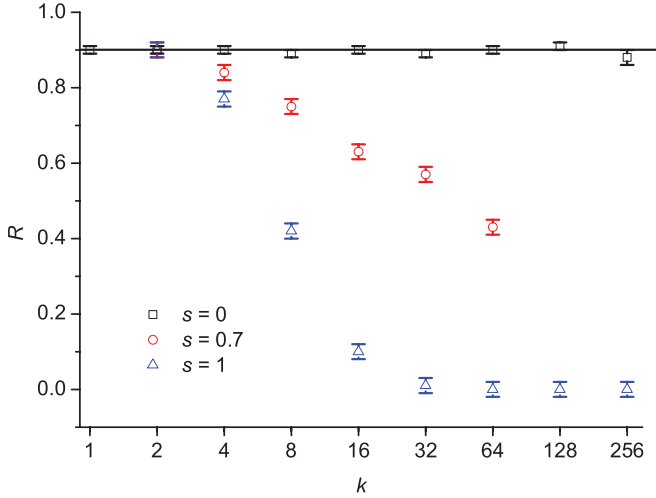


FIG. 7. (Color online) Intersection point of percolation probability  $R^*$  versus  $k$  at  $s = 0.0, 0.7, 1.0$ .

for the completely ordered systems ( $s = 1$ ), where the effect of the  $k$ -mer length on the value of  $R^*$  is maximal (Fig. 7). The more detailed analysis has shown that the structure of percolation clusters strongly depends upon  $k$ ; they have been elongated along vertical direction and the degree of elongation increased as length of  $k$ -mers increased (Fig. 8). Moreover, the mean degree of system anisotropy  $\delta$  calculated using Eq. (9) is dependent on  $k$ -mer concentration  $p$ , length  $k$ , and order parameter  $s$ .

Figure 9(a) presents examples of  $\delta$  versus order parameter  $s$  at different fixed concentrations  $p$  and fixed length of  $k$ -mer,  $k = 32$ . The size of lattice is relatively large,  $L = 4096$ , so, the finite size effects are rather small. For isotropic systems (at  $s = 0$ ), the value of  $\delta$  is always zero and it is maximal for completely ordered systems (at  $s = 1$ ). At small values of  $p$  the relation between  $\delta$  and  $s$  is nearly linear. With increasing of  $p$  and fixed  $s$  the value of  $\delta$  decreased; however, it noticeably dropped above percolation threshold and became practically zero in the vicinity of jamming concentration. For example, the concentration of  $p = 0.50$  is above the percolation threshold

TABLE I. Percolation threshold  $p_c$  versus order parameter  $s$  for  $k$ -mers of different length  $k$ . The errors are no larger than half a unit in the last place of the presented results.

| $s$ | $k = 2$ | $k = 4$ | $k = 8$ | $k = 16$ | $k = 32$ | $k = 64$ | $k = 128$ |
|-----|---------|---------|---------|----------|----------|----------|-----------|
| 0.0 | 0.5619  | 0.5050  | 0.4697  | 0.4638   | 0.4748   | 0.4928   | 0.5115    |
| 0.1 | 0.5621  | 0.5056  | 0.4702  | 0.4644   | 0.4751   | 0.4930   |           |
| 0.2 | 0.5627  | 0.5067  | 0.4717  | 0.4656   | 0.4763   | 0.4936   |           |
| 0.3 | 0.5638  | 0.5090  | 0.4742  | 0.4677   | 0.4777   | 0.4948   |           |
| 0.4 | 0.5653  | 0.5124  | 0.4777  | 0.4708   | 0.4802   | 0.4964   |           |
| 0.5 | 0.5672  | 0.5167  | 0.4825  | 0.4751   | 0.4834   | 0.4993   |           |
| 0.6 | 0.5698  | 0.5224  | 0.4890  | 0.4807   | 0.4879   | 0.5025   |           |
| 0.7 | 0.5728  | 0.5296  | 0.4977  | 0.4883   | 0.4939   | 0.5074   |           |
| 0.8 | 0.5765  | 0.5389  | 0.5092  | 0.4987   | 0.5021   | 0.5132   |           |
| 0.9 | 0.5809  | 0.5510  | 0.5251  | 0.5140   | 0.5142   | 0.5210   |           |
| 1.0 | 0.5862  | 0.5672  | 0.5526  | 0.5442   | 0.5397   | 0.5376   | 0.5366    |

for the systems with order parameter  $s$  below  $\simeq 0.8$  and, here, the  $\delta(s)$  dependence noticeably deviates from near linear [Fig. 9(a)]. Figure 9(b) presents examples of  $\delta$  versus order parameter  $s$  at different concentrations and fixed length of  $k$ -mer,  $k = 32$ , and the concentrations that corresponds to the percolation transitions for the given systems. The value of  $k$ -mer length  $k$  strongly affected the mean degree of the system anisotropy  $\delta$  at the percolation transition. For example, for dimers,  $k = 2$ , the value of  $\delta$  is rather small in the whole range of  $s$  between 0 and 1; however, with increasing of  $k$ , the  $\delta(s)$  has become more noticeable. We believe that they can transfer into the near-linear of type  $\delta \simeq s$  in the limit of large  $k$ -mer length,  $k \rightarrow \infty$ .

### B. Dependence of percolation threshold $p_c$ versus order parameter $s$

The  $p_c(s)$  dependencies for  $k$ -mers of different length ( $k = 2 \dots 128$ ) are presented in Fig. 10. For completeness, the precise numerical information is also collected in Table I. In addition, Table II presents rougher estimations for  $k = 256$  and  $k = 512$  for isotropic ( $s = 0$ ) and completely ordered ( $s = 1$ ) systems.

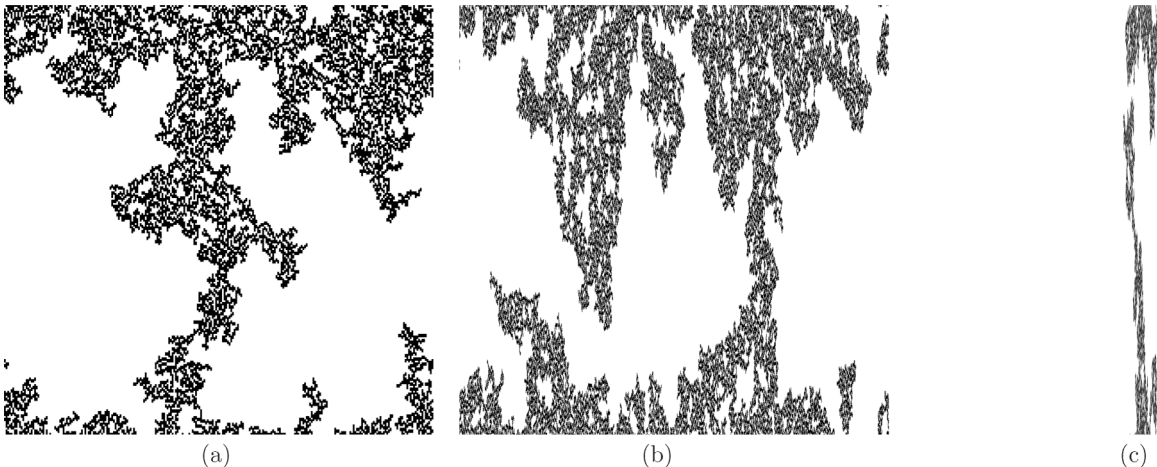


FIG. 8. Examples of wrapping clusters incipient in vertical direction for completely ordered system ( $s = 1.0$ ) for different length of  $k$ -mers. The size of a square lattice is  $L = 128k$ . Periodical boundary conditions. (a)  $k = 2$ ; (b)  $k = 8$ ; (c)  $k = 32$ .

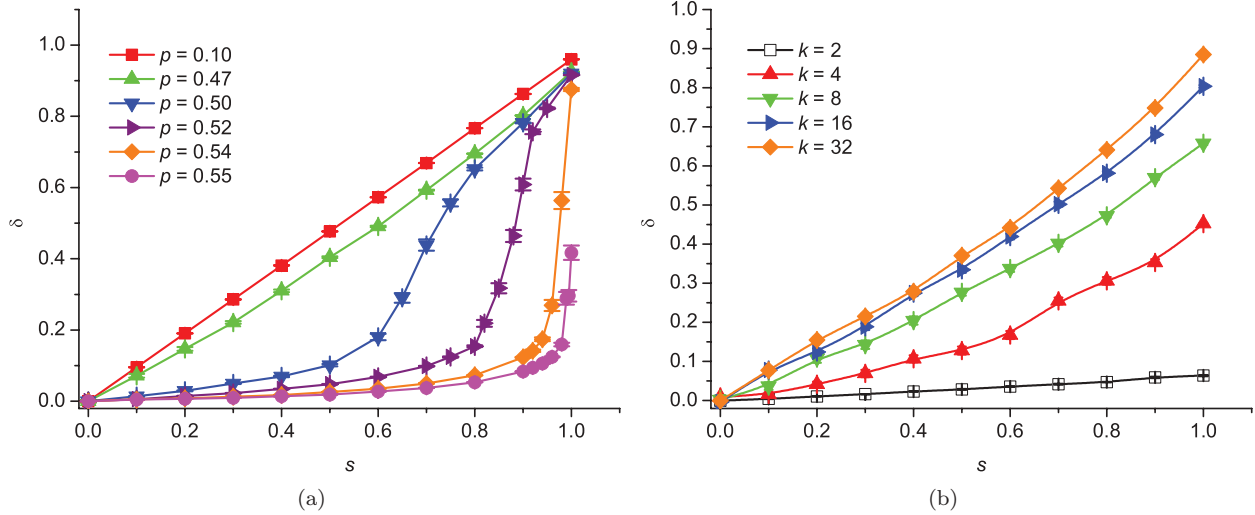


FIG. 9. (Color online) Mean degree of the system anisotropy  $\delta$  versus order parameter  $s$ : (a) at different concentrations  $p$  and the fixed length of a  $k$ -mer,  $k = 32$ ; (b) at different  $k$ -mer length  $k$  and concentrations that corresponds to the percolation transition for given systems. The size of lattice is  $L = 4096$  and the data averaged over 100 independent runs.

The obtained data evidence that the increase of system ordering always results in increase of  $p_c$  value. Such behavior correlates with theoretical results obtained for the systems of partially oriented penetrable rods [37–40] and experimentally studied effect of carbon nanotube alignment on percolation in polymer composites [41].

Figure 11 presents examples of  $p_c$  versus  $k$  dependencies obtained for different values of  $s$  in this work (1), as well as data presented earlier for the isotropic ( $s = 0$ ) and completely ordered ( $s = 1$ ): (2) Ref. [5], (3) Ref. [7], (4) Ref. [6], (5) Ref. [8], and (6) Ref. [13].

For completely ordered systems, i.e., at  $s = 1$ , the percolation threshold  $p_c$  monotonically decreased as value of  $k$  increased. Recently, the similar behavior for  $k$  from 1 to 12 with the asymptotic limit of  $p_c^\infty = p_c(k \rightarrow \infty) \simeq 0.54$  has been reported [13].

The analysis has shown that the data obtained in our work may be rather well fitted by the power function

$$p_c = a_1/k^{\alpha_1} + p_c^\infty, \quad (10)$$

where  $p_c^* = 0.533 \pm 0.001$ ,  $a_1 = 0.088 \pm 0.003$ ,  $\alpha_1 = 0.72 \pm 0.04$ , and  $r^2 = 0.998$  for the coefficient of determination.

We should note that for completely ordered penetrating anisotropic objects and continuous problem, the excluded volume theory predicts the absence of noticeable dependence of the percolation threshold on aspect ratio  $k$  [37,38]. In the lattice problem under consideration, observed effect of  $p_c(k)$

TABLE II. Estimations of percolation threshold  $p_c$  for  $k$ -mers of large length  $k$ . The errors are no larger than half a unit in the last place of the presented results.

| $s$ | $k = 256$ | $k = 512$ |
|-----|-----------|-----------|
| 0.0 | 0.530     | 0.5485    |
| 1.0 | 0.535     |           |

dependence may reflect the influence of the lattice discreteness on the percolation threshold.

In the problem under consideration, at  $s = 1$ , the formation of percolation cluster reflects the mode of connectivity between vertically oriented one-dimensional chains of  $k$ -mers. It may be assumed that in the limit of  $k \rightarrow \infty$  the connectivity of two  $k$ -mers in the neighboring vertical lines at their end sites is sufficient for a formation of percolation cluster with minimal concentration of  $p = 0.5$ , which is close to the numerically estimated value of  $p_c^* = 0.533 \pm 0.001$ .

In contrast, for partially ordered systems, i.e., at  $s < 1$ , the percolation threshold  $p_c$  is a nonmonotonic function of  $k$  and for a certain length of  $k$ -mers  $k = k_m$  a minimum of  $p_c$  has been observed (Fig. 11). In total, the data obtained in this work for isotropic systems (i.e., at  $s = 0$ ) have been in good correspondence with previously published data [5,7,8,13,42] with the only exception to those obtained for very long  $k$ -mers ( $k > 64$ ) in Ref. [42]. This inequality may reflect the relatively

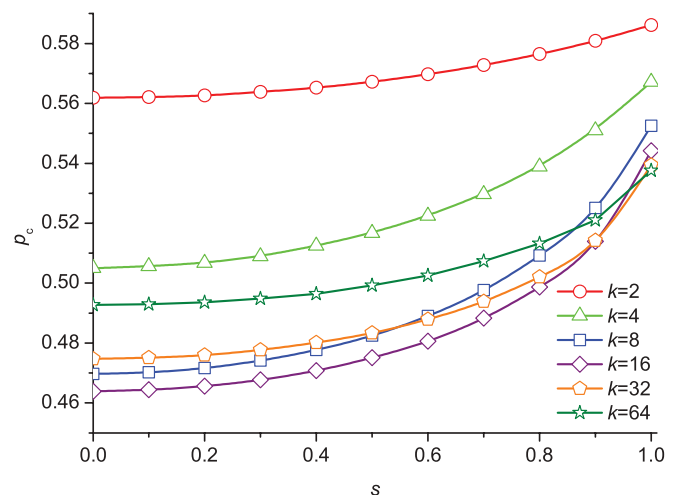


FIG. 10. (Color online) Percolation threshold  $p_c$  versus order parameter  $s$  for  $k$ -mers of different length.

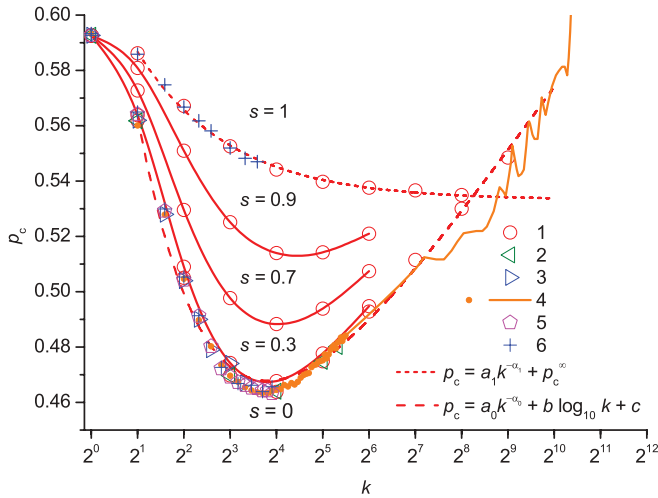


FIG. 11. (Color online) Percolation threshold  $p_c$  versus  $k$ -mer length  $k$  at different values of order parameter  $s$ . Here, the different data are presented that have been obtained in: (1) this work, (2) Ref. [5], (3) Ref. [7], (4) Ref. [6], (5) Ref. [8] and (6) Ref. [13]. The dashed lines have been obtained by least-square fitting of the data points using Eqs. [(10), (11)].

moderate size of lattices that has been used in Ref. [42] ( $L \leq 2500$ ), whereas in our simulations, the maximum size of the lattice is  $L \sim 100k$ , as a rule. In any case, our data confirmed the conclusion by Leroyer and Pommiers [5] and Kondrat and Pękalski [6] about the presence of minimum at the  $p_c$  versus  $k$  dependence. For the disordered systems the position of the minimum,  $k_m$ , is dependent on the value of  $s$ , e.g., it is  $k_m \simeq 13$  at  $s = 0$ ,  $k_m \simeq 16$  at  $s = 0.7$ ,  $k_m \simeq 22$  at  $s = 0.9$ , and it seems that  $k_m \rightarrow \infty$  in the limit of  $s \rightarrow 1$  (Fig. 11). We should note, that the asymptotic limit of  $p_c^* = p_c(k \rightarrow \infty) \simeq 0.461$  derived in Ref. [8] for  $s = 0$  in fact is very close to the value of  $p_c$  at point of minimum,  $k_m \simeq 13$ .

It is attractive to speculate that extremal  $p_c$  versus behavior for partially ordered systems may reflect the competition of

the two different effects influencing the value of percolation threshold. We tried to fit the obtained data for isotropic system ( $s = 0$ ) using the function

$$p_c = a_0/k^{\alpha_0} + b \log_{10} k + c \quad (11)$$

and obtained the following numerical estimations for the parameters  $a_0 = 0.36 \pm 0.02$ ,  $\alpha_0 = 0.81 \pm 0.12$ ,  $b = 0.08 \pm 0.01$ ,  $c = 0.33 \pm 0.02$ , and  $r^2 = 0.991$  for the coefficient of determination.

It is remarkable that exponents  $\alpha_0 = 0.81 \pm 0.12$  and  $\alpha_1 = 0.72 \pm 0.04$  are practically the same for  $s = 0$  and  $s = 1$ , respectively, and it may reflect the same effect of the discreteness on the percolation at the relatively small  $k$  ( $\leq 10$ ). For disordered systems, the logarithmic increase of  $p_c$  at large values of  $k$  [Eq. (11)] may reflect the tendency of  $k$ -mers for stacking, or formation of squarelike blocks, especially at large values of  $k$ . Such blocks of vertically and horizontally oriented  $k$ -mers are typical for partially ordered systems in jamming configurations [12]; however, they are also important at the percolation threshold. Examples of  $k$ -mer patterns ( $k = 128$ ) in the percolation point are presented in Fig. 12 for isotropic system ( $s = 0$ ). The sequential magnification of the system has shown the presence of rather compact blocks of vertically and horizontally oriented  $k$ -mers that have been connected into the percolating structure by overhanging of  $k$ -mers. The numerical studies have shown that for the ideal blocks, i.e.,  $k \times k$  squares, the percolation concentration increased and jamming concentration decreased as  $k$  value increased [43], and above certain critical value of  $k$  no percolation has been observed. In this situation, even at the saturation coverage (jamming), where no more object can be placed without any overlap, there exists only finite clusters of  $k \times k$  squares. We can assume the similar mechanism that governs the observed  $p_c \propto k$  increasing of percolation threshold. Leroyer and Pommiers used similar arguments for explanation of nonmonotonicity of percolation threshold [5]. A nonmonotonic  $p_c(k)$  behavior has been explained, accounting for the local alignment effects, which explains the change of structure of the critical clusters.

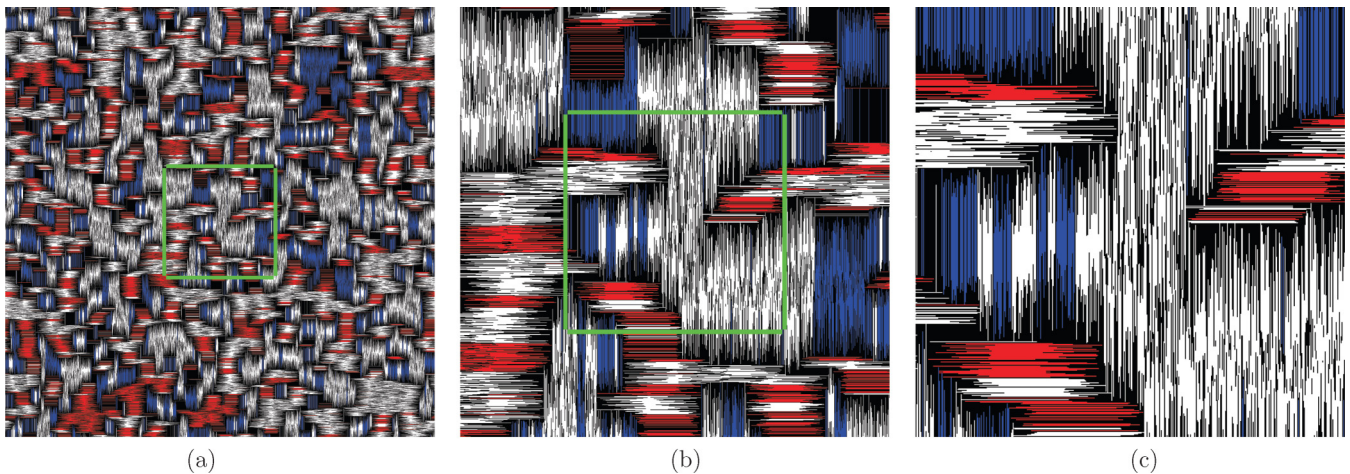


FIG. 12. (Color online) Examples of percolation configurations of  $k$ -mers ( $k = 128$ ) on a square lattice of size  $L = 4096$  at  $s = 0$ . Vertical and horizontal orientations are represented by different gray levels in printed version and in red and blue in online version; empty sites are labeled black and sites of percolation cluster are labeled white. Here, (a) shows the whole lattice; (b) shows the magnification of the pattern (a) in the central square; (c) shows the magnification of the pattern (b) in the central square.



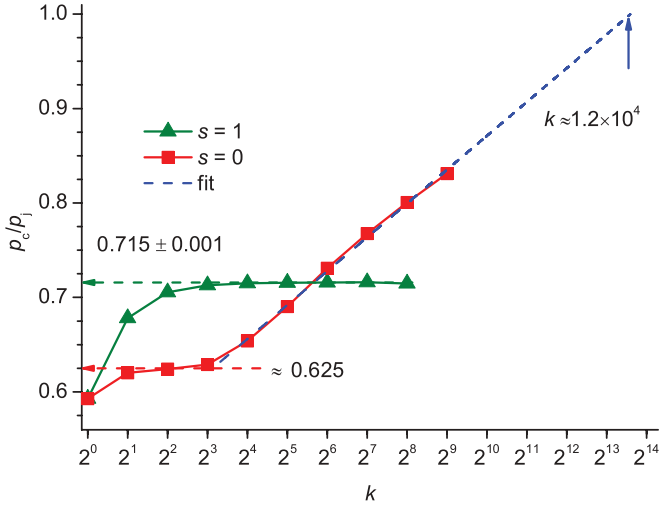


FIG. 13. (Color online) Ratio of percolation and jamming concentration  $p_c/p_j$  versus  $k$ -mer length  $k$  for disordered ( $s = 0$ ) and completely ordered  $s = 1$  systems. The dashed lines for  $s = 0$  have been obtained by least-square fitting of the data points using Eq. (12).

We checked the validity of conjecture of Vandewalle *et al.* [7] about the constancy of the ratio of percolation and jamming concentration  $p_c/p_j$  for disordered ( $s = 0$ ) and completely ordered  $s = 1$  systems (Fig. 13). The values of jamming concentration  $p_j$  have been taken from our previously published work [12]. For completely ordered systems ( $s = 1$ ), this ratio initially increased and became practically constant,  $p_c/p_j \simeq 0.715$ , at relatively large length of  $k$ -mers,  $k > 8$ .

For isotropic systems ( $s = 0$ ), this ratio is approximately constant only for small values of  $k$  ( $k = 2 \dots 8$ ). For larger  $k$ ,  $k = 16 \dots 256$ , the  $p_c/p_j$  increases proportionally to  $\log_{10} k$ :

$$p_c/p_j = b \log_{10} k + c, \quad (12)$$

where  $b = 0.119 \pm 0.003$  and  $c = 0.513 \pm 0.006$  are the constants. Our result is reasonably close to the estimation by Kondrat and Pękalski,  $b \simeq 0.13$  and  $c \simeq 0.50$  ( $15 \leq k \leq 45$ ) [6].

Thus, the constancy of the ratio  $p_c/p_j$  is true for the completely ordered systems ( $s = 1$ ). It may reflect a similar influence of the discreteness of the lattice on both jamming and percolation. On the other hand, the nonconstancy of the ratio  $p_c/p_j$  for isotropic systems ( $s = 0$ ) may reflect a different influence of the stacking on jamming and percolation. For this case, the approximation of the data presented in Fig. 13 gives  $p_c/p_j \simeq 1$  at  $k \simeq 1.2 \times 10^4$ . So, we can suppose that for very long  $k$ -mers, the percolation may be lost in close analogy with similar behavior observed for  $k \times k$  squares [43].

#### IV. CONCLUSION

In this paper, the percolation behavior of partially ordered linear  $k$ -mers on torus (square lattice with periodic boundary conditions) has been investigated by computer simulations. The length of a  $k$ -mer varies from 1 to 512 and different lattice sizes up to  $L = 1024k$  are used. The relaxation random sequential adsorption model [12] has been used to place the  $k$ -mers on a lattice. The alignment degree is characterized by order parameter  $s = 0 \dots 1$ :  $s = 0$  for isotropic system and  $s = 1$  for perfectly aligned system. The behavior of percolation cumulant at the intersection point  $R^*$  has been studied in detail in dependence on  $k$ ,  $s$ , and  $L$ . For isotropic problems, the value of position of intersection point remained unchanged within precision of estimation, being  $R^* \simeq 0.90$  for all studied length of  $k$ -mers. The universality of intersection points  $R^*$  (i.e., absence of dependence  $R^*$  of  $k$ ) has been observed only for isotropic systems,  $s = 0$ . This universality suggests that  $R^*$  can be derived from Ref. [31], not only for topological percolation but also for physical one. For anisotropic systems, this universality is violated and the value of  $R^*$  is dependent upon  $k$  and  $s$ . One can suppose that this violation can reflect the effect of the system anisotropy.

The increase of system ordering always results in an increase of percolation threshold  $p_c$ . The dependencies of  $p_c(k)$  for completely ordered ( $s = 1$ ) and partially ordered ( $s < 1$ ) systems are obviously different. For completely ordered systems, the percolation threshold  $p_c$  monotonically decreased as  $k$  increased. The power-law relation  $p_c \propto 1/k^{\alpha_1}$  ( $\alpha_1 = 0.72 \pm 0.04$ ) probably reflects effects of the lattice discreteness. For partially ordered systems, the percolation threshold  $p_c$  is always a nonmonotonic function of  $k$  and for a certain length of  $k$ -mers,  $k = k_m$ , a minimum of  $p_c$  has been observed. It has been assumed that this behavior may reflect the competition of the lattice discreteness (that is dominant at small values of  $k$ ) and the tendency of  $k$ -mers for stacking or formation of squarelike blocks (that is dominant at large values of  $k$ ). For completely ordered systems ( $s = 1$ ), the ratio of percolation and jamming concentration  $p_c/p_j$  is practically constant ( $p_c/p_j \simeq 0.715$ , at  $k > 8$ ). This behavior evidently reflects the presence of some universal connection in the geometry of percolation and jamming [7]. For isotropic systems ( $s = 0$ ), this ratio is not constant and increased proportionally to  $\log_{10} k$ .

Our simulations suggest that for  $s = 0$ , the percolation may be lost at  $k \gtrsim 1.2 \times 10^4$ . Additional investigation of percolation with extremely long objects should be performed in the future to confirm or reject this prediction.

#### ACKNOWLEDGMENT

This work is supported by the Ministry of Education and Science of Russia, Project No. 1.588.2011.

- [1] D. Stauffer and A. Aharony, *Introduction to Percolation Theory* (Taylor & Francis, London, 1992).  
 [2] M. Sahimi, *Application of Percolation Theory* (Taylor & Francis, London, 1994).

- [3] G. Grimmett, in *Lectures on Probability Theory and Statistics*, Lecture Notes in Mathematics, Vol. 1665 (Springer, Berlin/Heidelberg, 1997), pp. 153–300.  
 [4] J. Becklehimer and R. B. Pandey, *Physica A* **187**, 71 (1992).

- [5] Y. Leroyer and E. Pommiers, *Phys. Rev. B* **50**, 2795 (1994).
- [6] G. Kondrat and A. Pękalski, *Phys. Rev. E* **63**, 051108 (2001).
- [7] N. Vandewalle, S. Galam, and M. Kramer, *Eur. Phys. J. B* **14**, 407 (2000).
- [8] V. Cornette, A. J. Ramirez-Pastor, and F. Nieto, *Eur. Phys. J. B* **36**, 391 (2003).
- [9] V. Cornette, A. J. Ramirez-Pastor, and F. Nieto, *J. Chem. Phys.* **125**, 204702 (2006).
- [10] V. Cornette, A. J. Ramirez-Pastor, and F. Nieto, *Phys. Lett. A* **353**, 452 (2006).
- [11] V. A. Cherkasova, Y. Y. Tarasevich, N. I. Lebovka, and N. V. Vygornitskii, *Eur. Phys. J. B* **74**, 205 (2010).
- [12] N. I. Lebovka, N. N. Karmazina, Y. Y. Tarasevich, and V. V. Laptev, *Phys. Rev. E* **84**, 061603 (2011).
- [13] P. Longone, P. M. Centres, and A. J. Ramirez-Pastor, *Phys. Rev. E* **85**, 011108 (2012).
- [14] A. Ghosh and D. Dhar, *Europhys. Lett.* **78**, 20003 (2007).
- [15] D. A. Matoz-Fernandez, D. H. Linares, and A. J. Ramirez-Pastor, *Physica A* **387**, 6513 (2008).
- [16] D. A. Matoz-Fernandez, D. H. Linares, and A. J. Ramirez-Pastor, *J. Chem. Phys.* **128**, 214902 (2008).
- [17] D. A. Matoz-Fernandez, D. H. Linares, and A. J. Ramirez-Pastor, *Langmuir* **27**, 2456 (2011).
- [18] D. A. Matoz-Fernandez, D. H. Linares, and A. J. Ramirez-Pastor, *Eur. Phys. J. B* **85**, 1 (2012).
- [19] S. Žerko, P. Polanowski, and A. Sikorski, *Soft Matter* **8**, 973 (2012).
- [20] A. V. Kyrlyuk and P. van der Schoot, *Proc. Nat. Acad. Sci. USA* **105**, 8221 (2008); **105**, 11451 (2008).
- [21] Y. Ma, B. Wang, Y. Wu, Y. Huang, and Y. Chen, *Carbon* **49**, 4098 (2011).
- [22] L. Gao, X. Zhou, and Y. Ding, *Chem. Phys. Lett.* **434**, 297 (2007).
- [23] Y. Pan, G. J. Weng, S. A. Meguid, W. S. Bao, Z.-H. Zhu, and A. M. S. Hamouda, *J. Appl. Phys.* **110**, 123715 (2011).
- [24] L. Vovchenko and V. Vovchenko, *Materialwissenschaft und Werkstofftechnik* **42**, 70 (2011).
- [25] A. V. Kyrlyuk, M. C. Hermant, T. Schilling, B. Klumperman, C. E. Koning, and P. van der Schoot, *Nat. Nano* **6**, 364 (2011).
- [26] F. Carmona, F. Barreau, P. Delhaes, and R. Canet, *J. Phys. Lett.* **41**, 531 (1980).
- [27] T. W. Noh, S.-I. Lee, Y. Song, and J. Gaines, *Phys. Lett. A* **114**, 207 (1986).
- [28] K. H. Han, J. O. Lee, and S.-I. Lee, *Phys. Rev. B* **44**, 6791 (1991).
- [29] M. Matsumoto and T. Nishimura, *ACM Trans. Model. Comput. Simul.* **8**, 3 (1998).
- [30] G. Pruessner and N. R. Moloney, *J. Phys. A* **36**, 11213 (2003).
- [31] H. Pinson, *J. Stat. Phys.* **75**, 1167 (1994).
- [32] M. E. J. Newman and R. M. Ziff, *Phys. Rev. Lett.* **85**, 4104 (2000).
- [33] M. E. J. Newman and R. M. Ziff, *Phys. Rev. E* **64**, 016706 (2001).
- [34] R. M. Ziff and R. D. Vigil, *J. Phys. A* **23**, 5103 (1990).
- [35] M. D. Rintoul and S. Torquato, *J. Phys. A* **30**, L585 (1997).
- [36] J. Hoshen and R. Kopelman, *Phys. Rev. B* **14**, 3438 (1976).
- [37] I. Balberg and N. Binenbaum, *Phys. Rev. B* **28**, 3799 (1983).
- [38] I. Balberg, N. Binenbaum, and C. H. Anderson, *Phys. Rev. Lett.* **51**, 1605 (1983).
- [39] W. J. Boudville and T. C. McGill, *Phys. Rev. B* **39**, 369 (1989).
- [40] T. Natsuki, M. Endo, and T. Takahashi, *Physica A* **352**, 498 (2005).
- [41] F. Du, J. E. Fischer, and K. I. Winey, *Phys. Rev. B* **72**, 121404 (2005).
- [42] G. Kondrat, *J. Chem. Phys.* **117**, 6662 (2002).
- [43] M. Nakamura, *Phys. Rev. A* **36**, 2384 (1987).